

See discussions, stats, and author profiles for this publication at: <https://www.researchgate.net/publication/231409413>

# Unimolecular decay lifetimes and intramolecular energy redistribution in hydrogen peroxide: sensitivity to potential energy surface

ARTICLE *in* THE JOURNAL OF PHYSICAL CHEMISTRY · MAY 1989

Impact Factor: 2.78 · DOI: 10.1021/j100347a001

---

CITATIONS

26

---

READS

5

4 AUTHORS, INCLUDING:



**Bobby Sumpter**

Oak Ridge National Laboratory

452 PUBLICATIONS 7,671 CITATIONS

SEE PROFILE



**Jesus Santamaria**

Complutense University of Madrid

37 PUBLICATIONS 365 CITATIONS

SEE PROFILE

## LETTERS

### Unimolecular Decay Lifetimes and Intramolecular Energy Redistribution in HOOH: Sensitivity to Potential Energy Surface

Coral Getino,<sup>†</sup> Bobby G. Sumpter,<sup>‡</sup> Jesus Santamaria,<sup>†</sup> and Gregory S. Ezra<sup>\*,§</sup>

Baker Laboratory, Department of Chemistry, Cornell University, Ithaca, New York 14853

(Received: January 18, 1989)

Quasiclassical trajectory calculations of unimolecular dissociation lifetimes following OH local mode overtone absorption in hydrogen peroxide are reported for  $\nu_{\text{OH}} = 6$  and 7. Both nonrotating and rotating ( $E_{\text{rot}} = 300$  K) ensembles are considered. For  $\nu_{\text{OH}} = 6$ , our potential surface yields dissociation lifetimes of 20–25 ps, considerably longer than the values 5–6 ps inferred from spectroscopic line widths. Quasiclassical overtone relaxation rates calculated on the same potential surface are however consistent with observed overtone line widths. For both  $\nu_{\text{OH}} = 6$  and 7, a marked separation in time scales between overtone relaxation and unimolecular decay is found.

#### Introduction

There is currently much interest in obtaining information on intramolecular and unimolecular decay dynamics from local mode overtone spectroscopy.<sup>1</sup> Measurement of homogeneous line widths<sup>1,2</sup> and homogeneous structure<sup>3</sup> can yield information on time scales for intramolecular vibrational redistribution and/or unimolecular dissociation. Knowledge of the latter as a function of initial state energy and angular momentum can provide detailed tests of current statistical theories of unimolecular reaction rates.<sup>4</sup>

The OH local mode spectroscopy and overtone-induced unimolecular dissociation of HOOH into OH fragments have been the subject of several experimental<sup>5–13</sup> and theoretical<sup>6,9,14–19</sup> investigations. Except for the recent work of Zewail and co-workers on thermally assisted dissociation,<sup>10</sup> the experiments to date have not measured the rate of appearance of products directly. Lower bounds to unimolecular decay lifetimes have been inferred from

measured homogeneous overtone line widths by using the inequality

$$\tau_{\text{line width}} \leq \tau_{\text{unimolecular}} \quad (1)$$

(1) Crim, F. F. *Annu. Rev. Phys. Chem.* **1984**, *35*, 657. Uzer, T. *Adv. At. Mol. Phys.* **1988**, *25*, 417. Berry, M. J. *Proc. Conf. Robert A. Welch Foundation Chem. Res.* **1985**, XXVIII.

(2) Gentry, W. R. *Resonances in Electron-Molecule Scattering, van der Waals Complexes and Reactive Chemical Dynamics*; Truhlar, D. G., Ed.; American Chemical Society: Washington, DC, 1984; Symp. Ser. No. 263, p 289. *Structure and Dynamics of Weakly-bound Systems*; Weber, A., Ed.; Reidel: Dordrecht, 1987.

(3) See: Puttkamer, K. v.; Dubal, H.-R.; Quack, M. *Faraday Discuss. Chem. Soc.* **1983**, *75*, 197. Quack, M. *J. Chem. Soc., Faraday Trans. 2* **1988**, *84*, 1626.

(4) Robinson, P. J.; Holbrook, K. A. *Unimolecular Reactions*; Wiley: New York, 1972. Forst, W. *Theory of Unimolecular Reactions*; Academic: New York, 1973.

(5) Rizzo, T. R.; Hayden, C. C.; Crim, F. F. *Faraday Discuss. Chem. Soc.* **1983**, *75*, 112. Rizzo, T. R.; Hayden, C. C.; Crim, F. F. *J. Chem. Phys.* **1984**, *81*, 4501.

(6) Dubal, H.-R.; Crim, F. F. *J. Chem. Phys.* **1985**, *83*, 3863.

(7) Ticich, T. M.; Rizzo, T. R.; Dubal, H.-R.; Crim, F. F. *J. Chem. Phys.* **1986**, *84*, 1508.

<sup>†</sup> Permanent address: Departamento de Química-Física, Facultad de CC. Químicas, Universidad Complutense, 28040 Madrid, Spain.

<sup>‡</sup> Present address: Chemistry Division, Oak Ridge National Laboratory, Oak Ridge, TN 37831.

<sup>§</sup> Alfred P. Sloan Fellow; Camille and Henry Dreyfus Teacher-Scholar.

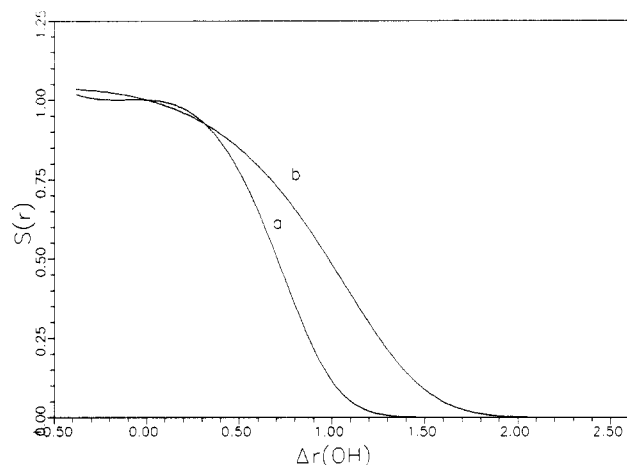


**Figure 1.** Switching functions  $S(r_{\text{OH}})$  describing the attenuation of the HOO bend force constant with stretching of the OH bond: (a) present work (cf. ref 21 and 22); (b) ref 14.

Unimolecular dissociation rates previously calculated by Uzer et al.<sup>14</sup> (classical trajectory), Brouwer et al. (statistical adiabatic channel),<sup>9</sup> and Sumpter and Thompson (trajectory and Monte Carlo statistical)<sup>15</sup> are consistent with lifetimes in the range 3.5–7.0 ps for  $\nu_{\text{OH}} = 6$  inferred from experimental spectra<sup>8,11</sup> on the assumption that the dominant contribution to the overtone line width is due to unimolecular decay.

The potential energy surface used in the trajectory calculations of Uzer et al.<sup>14</sup> incorporated spectroscopic and thermodynamic data and modeled the OH and OO bond stretches as Morse oscillators and the HOO bends as harmonic oscillators. (Torsional motion was frozen in the majority of the calculations reported in ref 14.) Potential coupling between the zeroth-order modes was introduced in two ways: off-diagonal terms in the F-matrix and switching functions describing the attenuation of the HOO harmonic bend force constant by stretching of the adjacent HO or OO bond.<sup>20–22</sup>

The potential surface of Uzer et al. was however unsatisfactory in several respects (as noted by these authors<sup>14</sup>). The switching functions used in ref 14 actually describe stretch–bend potential coupling in a CCH fragment;<sup>20</sup> switching functions appropriate for the OOH fragment have since become available.<sup>21,22</sup> In addition, the off-diagonal F-matrix elements exhibit unphysical behavior at large values of the OO bond length, as they are not attenuated in a physically appropriate fashion as the molecule falls apart. Apart from its effect on the dynamics, this unphysical asymptotic behavior of the potential means that it is not possible

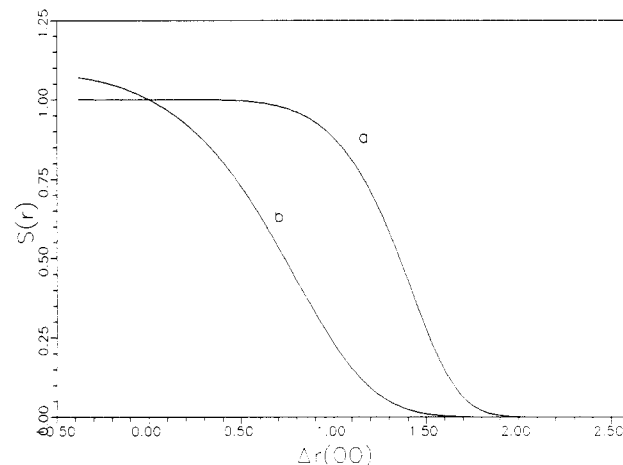


**Figure 2.** Switching functions  $S(r_{\text{OO}})$  describing the attenuation of the HOO bend force constant with stretching of the OO bond: (a) present work; (b) ref 14.

**TABLE I: Quasiclassical Overtone Line Widths, Associated Relaxation Times and Unimolecular Decay Lifetimes for Overtone Excited HOOH**

$\nu_{\text{OH}}$	line width, $\text{cm}^{-1}$	$\tau$ , ps	$\tau_{\text{unimolecular}}$ , ps
4	0.009 <sup>a</sup> (0.009) <sup>b</sup>	589 (589)	
5	0.05 (0.05)	106 (106)	
6	0.71 (0.49)	7.50 (10.8)	20.9 (24.9)
7	4.0 (3.5)	1.3 (1.5)	9.9 (12.3)

<sup>a</sup> Ensemble of molecules with rotational energy equivalent to  $T = 300$  K. <sup>b</sup> Ensemble of nonrotating molecules.

to obtain well-defined rotation–vibration state distributions of the OH fragments for comparison with experiment.<sup>5</sup>

In this Letter we present results of quasiclassical trajectory calculations of overtone-induced unimolecular decay of HOOH using a potential surface in which the above shortcomings have been corrected. We also examine the relation between the time scale for classical unimolecular decay and that for intramolecular vibrational energy redistribution.

### Potential Energy Surface for HOOH

In brief, the potential surface used here (cf. ref 23; further details and trajectory results for other model surfaces are given in ref 19) is an ab initio/empirical surface of the form used by Uzer et al.,<sup>14</sup> in which the deficiencies noted above have been remedied.

First, the potential behaves in a physically reasonable fashion as  $r_{\text{OO}} \rightarrow \infty$ . Thus, off-diagonal harmonic force field potential coupling terms are fit to a sum of nonbonded Lennard-Jones interactions, which decay to zero as  $r_{\text{OO}} \rightarrow \infty$ . In addition, the OH bond force constants relax to their values for free OH, and the torsional potential is represented as a Fourier series with coefficients that go to zero as the molecule dissociates.<sup>19,23</sup>

Second, ab initio calculations (SCF with 6-31G\*\* basis using the GAUSSIAN package<sup>24</sup>) have been used to determine the switching function  $S(r_{\text{OO}})$  that determines the potential energy coupling between the HOO bend and the reaction coordinate. The function used has the form

$$S(r_{\text{OO}}) = 1 - \tanh(0.12505\Delta r_{\text{OO}}^5) \quad (2)$$

The switching function  $S(r_{\text{OH}})$  describing the attenuation of the HOO bend force constant by the OH stretch is that given in ref 22.

The switching functions are plotted in Figures 1 and 2, together with the switching functions used in ref 14. For both the OH and OO stretches, there are appreciable differences between the two functions. Since the stretch–bend coupling induced by the

(8) Butler, L. J.; Ticich, T. M.; Likar, M. D.; Crim, F. F. *J. Chem. Phys.* **1986**, *85*, 2331.

(9) Brouwer, L.; Cobos, C. J.; Troe, J.; Dubal, H.-R.; Crim, F. F. *J. Chem. Phys.* **1987**, *86*, 6171.

(10) Scherer, N. F.; Doany, F. E.; Zewail, A. H.; Perry, J. W. *J. Chem. Phys.* **1986**, *84*, 1932. Scherer, N. F.; Zewail, A. H. *J. Chem. Phys.* **1987**, *87*, 97.

(11) Luo, X.; Rieger, P. T.; Perry, D. S.; Rizzo, T. R. *J. Chem. Phys.* **1988**, *89*, 4448.

(12) Ticich, T. M.; Likar, M. D.; Dubal, H.-R.; Butler, L. J.; Crim, F. F. *J. Chem. Phys.* **1987**, *87*, 5820.

(13) Douketis, C.; Reilly, J. P. Presented at the 3rd International Laser Science Conference, Atlantic City, NJ, 1987.

(14) Uzer, T.; Hynes, J. T.; Reinhardt, W. P. *Chem. Phys. Lett.* **1985**, *117*, 600; *J. Chem. Phys.* **1986**, *85*, 5791.

(15) Sumpter, B. G.; Thompson, D. L. *J. Chem. Phys.* **1985**, *82*, 4557; *J. Chem. Phys.* **1987**, *86*, 2805; *Chem. Phys. Lett.* **1988**, *153*, 243.

(16) Carpenter, J. E.; Weinhold, F. *J. Phys. Chem.* **1988**, *92*, 4295, 4306; **1986**, *90*, 6405.

(17) Nishikawa, A.; Lin, S. H. *Chem. Phys. Lett.* **1988**, *149*, 243.

(18) Uzer, T.; MacDonald, B. D.; Guan, Y.; Thompson, D. L. *Chem. Phys. Lett.* **1988**, *152*, 405.

(19) Getino, C.; Sumpter, B. G.; Santamaria, J.; Ezra, G. S. To be submitted for publication.

(20) Duchovic, R.; Hase, W. L.; Schlegel, H. B. *J. Chem. Phys.* **1984**, *88*, 1339.

(21) Wolf, R. J.; Bhatia, D. S.; Hase, W. L. *Chem. Phys. Lett.* **1986**, *132*, 493.

(22) Lemon, W. J.; Hase, W. L. *J. Phys. Chem.* **1987**, *91*, 1596.

(23) Sumpter, B. G. Ph.D. Thesis, Oklahoma State University, 1986.

(24) Hehre, W. J.; Radom, L.; Schleyer, P. v. R.; Pople, J. A. *Ab Initio Molecular Orbital Theory*; Wiley: New York, 1986.

switching functions is important in determining the rate and extent of intramolecular vibrational energy flow, the precise form of the couplings is likely to be of crucial significance for the dissociation dynamics.

### Unimolecular Dissociation Lifetimes

For the potential surface just described, we have calculated using standard quasiclassical trajectory techniques<sup>25</sup> both unimolecular dissociation lifetimes and OH fragment state distributions following excitation of OH local mode overtone states with  $\nu_{\text{OH}} = 6$  and 7. The quasiclassical sampling of vibrational phase space corresponded to an initial nonstationary state with a given number of OH local mode quanta and zero-point energy in the rest of the molecule.<sup>19,25</sup> Both nonrotating and rotating ( $T = 300$  K) ensembles were used. For  $\nu_{\text{OH}} = 6$  plus thermal rotation, OH fragment rotation-vibration state distributions were found to be in satisfactory agreement with experiment.<sup>5</sup> (Neither product state distributions nor unimolecular decay lifetimes were used to constrain the potential parameters.)

Unimolecular decay lifetimes for  $\nu_{\text{OH}} = 6$  and 7 for ensembles of 100 trajectories are given in Table I. Lifetimes for  $\nu_{\text{OH}} = 6$  obtained with the present potential are of the order of 20–25 ps, considerably longer than those reported in earlier calculations.<sup>9,14,15</sup> The dissociation lifetimes for the rotating ensembles are noticeably shorter than those for the nonrotating ensembles. The unimolecular decay lifetimes for  $\nu_{\text{OH}} = 6$  and 7 are clearly sensitive to details of the potential surface, in particular the precise form of the switching functions used to describe stretch-bend potential coupling (cf. Figures 1 and 2).

While our lifetimes for  $\nu_{\text{OH}} = 6$  are certainly consistent with the latest experimental data<sup>11</sup> (cf. the condition given in eq 1), the lifetimes we obtain imply a contribution to the homogeneous line width of 0.2–0.25  $\text{cm}^{-1}$  and so are unable to account for the observed  $\nu_{\text{OH}} = 6$  line widths.<sup>11</sup> In addition to the question of sensitivity of dynamics to potential surface,<sup>26</sup> our findings also raise the fundamental problem of the precise relation between homogeneous line widths and dissociation rates.<sup>2</sup>

The detailed mechanism for HOOH dissociation on the potential surface used here will be discussed elsewhere.<sup>19</sup>

### Time Scales for IVR versus Unimolecular Decay

The classical trajectory method enables us to investigate time scales for intramolecular vibrational energy redistribution (IVR) in addition to unimolecular decay times (cf. Figure 17 of ref 14). Using the quasiclassical prescription of Lu and Hase (ref 27, see also ref 28), it is possible to obtain an effective line width/time scale associated with relaxation of the initially excited local mode state and to compare the resulting overtone relaxation time scale with the unimolecular decay lifetimes calculated for the same potential surface and with experimental homogeneous line widths.<sup>11</sup>

If the probability of remaining in the initial state with  $n$  quanta in the OH bond is  $P_n(t)$ , the quasiclassical approximation to the low-resolution absorption intensity at a frequency displaced by  $\omega$  from the center of the overtone band is<sup>27,28</sup>

$$I(\omega) \propto \int_0^\infty dt \exp(i\omega t) c_n(t) \quad (3)$$

where

$$c_n(t) = P_n(t)^{1/2} \quad (4)$$

A quasiclassical initial sampling of phase space for a state with a given number of OH local mode quanta is used to calculate  $P_n(t)$ , corresponding to a bond dipole approximation.

The quasiclassical survival probability time series used to calculate  $I(\omega)$  from eq 3 are only a few picoseconds long, and use of conventional FFT routines<sup>29</sup> to evaluate the integral  $I(\omega)$  gives

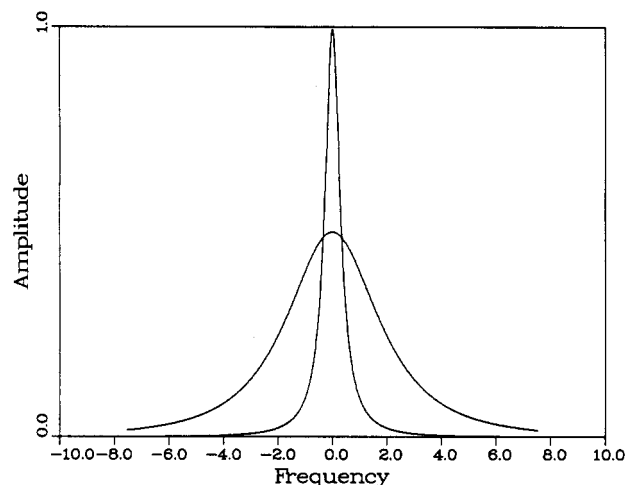


Figure 3. Quasiclassical overtone absorption line shapes calculated via eq 3 (cf. ref 27). Frequency units are wavenumbers ( $\text{cm}^{-1}$ ), measured from the center of the absorption peak. The narrow line corresponds to  $\nu = 6$ , while the broad line corresponds to  $\nu = 7$ . Both trajectory ensembles have  $E_{\text{rot}} = 300$  K. Relative intensities have no significance.

unacceptably low frequency resolution. We have therefore used the MUSIC spectral estimator<sup>30,31</sup> to obtain quasiclassical line widths; tests on a series of exponentially decaying functions showed that MUSIC is capable of computing accurate Fourier transforms using relatively short time series.

Our results are given in Table I for ensembles of 100 trajectories with 300 K of rotational energy. Quasiclassical simulation of the low-resolution overtone spectrum yields the effective line widths shown in Table I (cf. Figure 3); these line widths are converted into IVR times via

$$\tau = 1/\Delta\omega 2\pi c \quad (5)$$

where  $\Delta\omega$  is the fwhm of the absorption line.

For the potential used here, the trajectory results show very clearly a marked separation in time scales (more than a factor of 2) between overtone relaxation and unimolecular decay for  $\nu_{\text{OH}} = 6$  and 7. Such a separation of time scales was also found in ref 14. Detailed examination of classical trajectories<sup>14,19</sup> shows that energy initially in an excited local mode does not flow directly from the OH bond into the reaction coordinate (OO bond) but accumulates in the OO bond only relatively slowly. The separation of time scales found here reflects the sequential nature of the classical unimolecular dissociation.

Overtone relaxation rates for the nondissociating states  $\nu_{\text{OH}} = 4$  and 5 are also shown in Table I. (A small number of trajectories dissociate for these states as a consequence of "adiabatic leak".<sup>32</sup> The classical trajectory results indicate that initial energy flow out of the excited OH bond is very much slower for  $\nu_{\text{OH}} = 4$  and 5. For  $\nu_{\text{OH}} = 6$ , the excited OH bond is initially in a 5:2 Fermi resonance with the adjacent bend;<sup>19</sup> a low-order resonance is not present for  $\nu_{\text{OH}} = 4$  and 5.

We note that the quasiclassical effective overtone line width calculated for an ensemble of rotating molecules with  $\nu_{\text{OH}} = 6$  ( $0.71 \text{ cm}^{-1}$ ) is in strikingly good agreement with the very recent experimental result ( $0.8 \text{ cm}^{-1}$ ) of Luo et al. for the rotational state  $(J, K) = (12, 2)$ .<sup>11</sup> Such agreement is in all probability entirely fortuitous. In addition to uncertainties concerning both the potential surface and the dipole surface, where the latter determines the nature of the initially prepared state, the quasiclassical approximation for calculating line shapes is of dubious validity in the present context. A necessary condition for the quasiclassical procedure to yield a reasonable approximation to the envelope

(25) Raff, L. M.; Thompson, D. L. In *Theory of Chemical Reaction Dynamics*; Baer, M., Ed.; CRC Press: Boca Raton, FL, 1985.

(26) Hase, W. L. *J. Phys. Chem.* **1986**, *90*, 365.

(27) Lu, D.-H.; Hase, W. L. *J. Phys. Chem.* **1988**, *92*, 3217.

(28) Davis, M. J.; Heller, E. J. *J. Phys. Chem.* **1980**, *84*, 1999.

(29) Oran Brigham, E. *The Fast Fourier Transform*; Prentice-Hall: Englewood Cliffs, NJ, 1975.

(30) Marple, S. L. *Digital Spectral Analysis with Applications*; Prentice-Hall: Englewood Cliffs, NJ, 1987.

(31) Noid, D. W.; Broocks, B. T.; Gray, S. K.; Marple, S. L. *J. Phys. Chem.* **1988**, *92*, 3386. Noid, D. W.; Gray, S. K. *Chem. Phys. Lett.* **1988**, *145*, 9.

(32) Schatz, G. C. *J. Chem. Phys.* **1983**, *79*, 5386.

of a quantum spectrum is that the density of vibrational quantum states should be sufficiently large. Hydrogen peroxide is however close to the small molecule limit, in which case IVR gives rise to homogeneous structure in the spectrum rather than homogeneous broadening.<sup>3</sup> The only possible source of truly homogeneous line width in this limit is coupling to the dissociative continuum. An accurate value for the vibrational density of states of HOOH at the energy of the  $\nu_{\text{OH}} = 6$  state is not currently available.

### Conclusions

We have reported the results of classical trajectory studies of overtone-induced dissociation and IVR in HOOH using a potential energy surface of the type constructed by Uzer et al.,<sup>14</sup> in which several of the deficiencies noted by the latter authors have been remedied.

Our calculations yield unimolecular decay lifetimes for  $\nu_{\text{OH}} = 6$  in the range 20–25 ps, considerably larger than currently accepted values. These results demonstrate the sensitivity of the dissociation lifetime to details of the potential surface and point up the need for accurate ab initio calculations of the HOOH

potential surface, as well as direct measurements of the rate of appearance of OH fragments following overtone excitation.

We have also calculated effective quasiclassical overtone line widths using the prescription of ref 27. These line widths are determined by the relatively rapid relaxation of the initially excited overtone, rather than by the unimolecular decay rate. In the small molecule limit, the quantum manifestation of IVR following overtone excitation is homogeneous structure rather than homogeneous broadening.<sup>3</sup> Individual eigenstates are homogeneously broadened by coupling to the dissociative continuum, and in this case classical mechanics is of questionable utility for calculating overtone line shapes.

**Acknowledgment.** It is a pleasure to thank Profs. F. F. Crim, J. T. Hynes, T. Rizzo, M. Shapiro, and T. Uzer for helpful discussions and comments. This work was supported by NSF Grant CHE-8704632 and by the U.S.–Spain Cooperative Program in Basic Sciences. Computations reported here were performed on the Cornell National Supercomputer Facility, which is supported by the NSF and IBM Corporation.

## Femtosecond Dynamics of Geminate Pair Recombination in Pure Liquid Water

Y. Gauduel,\* S. Pommeret, A. Migus, and A. Antonetti

Laboratoire d'Optique Appliquée-INSERM U275, Ecole Polytechnique-ENS Techniques Avancées, 91120 Palaiseau, France (Received: January 30, 1989)

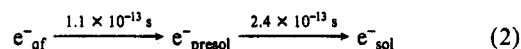
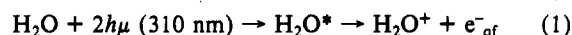
The dynamic behavior of the hydrated electron generated by two-photon ionization of pure liquid water has been investigated by using femtosecond laser spectroscopy. An early decay of the red-induced absorption has been observed in the first 100 ps following the energy deposition and is assigned to the geminate pair recombination  $\text{H}_3\text{O}^+ \cdots e_{\text{aq}}^-$  or  $\text{OH} \cdots e_{\text{aq}}^-$ .

The ultrafast reactivities of ions and radicals upon pulse radiolysis or photolysis of aqueous media are of fundamental importance in radiation chemistry and biology. In particular the direct assessment of the initial time dependence of transient radical populations following interaction of radiation with condensed matter should permit an understanding of the primary reactions occurring after energy deposition in the medium.<sup>1</sup>

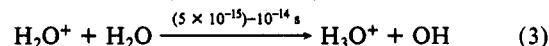
Experimental pulse radiolysis of aqueous media have been extensively performed to investigate the fate of spatial distribution of primary radical species ( $e_{\text{aq}}^-$ ,  $\text{H}_2\text{O}^+$ ,  $\text{H}_3\text{O}^+$ , OH, H) in tracks or spurs.<sup>2–4</sup> More precisely, the understanding of ultrafast reactions such as geminate ion pair recombinations requires a knowledge of the initial distribution of species inside the polar liquid. Indeed, the experimental investigation of ultrafast radical reactions in polar media provides information to test the validity of the models of stochastic processes in nonhomogeneous reactions by using Monte Carlo techniques or mechanical statistics.<sup>5–7</sup> However, the picosecond barrier in pulse radiolysis experiments has up to now prevented the direct investigation of such ultrafast radical reactions.

Advances in short-pulse optical measurement techniques have pushed this limit toward the femtosecond regime allowing us to investigate the primary events following energy deposition in polar liquids. Femtosecond photochemistry is a powerful method to study an electron–ion pair in pure aqueous media. During the interaction of high-power femtosecond UV pulses ( $I \approx 10^{12}$  W/cm<sup>2</sup>) with liquid water, the absorption of energy initiates the photodetachment of epithermal electrons with a small excess kinetic energy.<sup>8–10</sup> Recent femtosecond photolysis experiments in pure liquid water at ambient temperature have shown that the initial energy deposition in the bulk phase is followed, within 0.3

ps, by the electron thermalization, trapping, and solvation processes (reactions 1 and 2). The cation radical of water ( $\text{H}_2\text{O}^+$ ) un-



dergoes simultaneously a ultrafast proton reaction with one of the surrounding molecules. This charge transfer is believed to take place in less than  $5 \times 10^{-15}$  to  $10^{-14}$  s,<sup>1</sup> leading to the formation of the hydrogen ion  $\text{H}_3\text{O}^+$  and the hydroxyl radical OH (reaction 3). These two nearest neighbors ( $\text{H}_3\text{O}^+$ , OH) are produced earlier



than the electron solvation.<sup>11</sup> The initial spatial distribution of electron–ion pair and the high rate constants of the reactions of

(1) Magee, J. L.; Chatterjee, A. In *Radiation Chemistry*, Farhataziz and Rodgers, Eds.; VCH: New York, 1987; p 137.

(2) Jonah, C. D.; Matheson, M. S.; Miller, J. R.; Hart, E. J. *J. Phys. Chem.* **1976**, *80*, 1267.

(3) Chernovitz, A. C.; Jonah, C. D. *J. Phys. Chem.* **1988**, *92*, 5946.

(4) Freeman, G. R. In *Kinetics of Nonhomogeneous Processes*; Freeman, G. R., Ed.; Wiley: New York, 1987; p 277.

(5) Mozumder, A.; Magee, J. L. *Radiat. Res.* **1966**, *20*, 203.

(6) Mozumder, A. *Radiat. Res.* **1985**, *104*, 33.

(7) Clifford, P.; Green, N. J. B.; Pilling, M. J. *J. R. Statist. Soc. B* **1987**, *49*, 266 and references therein.

(8) Nikogozyan, D. N.; Oraevsky, A. A.; Rupasov, V. I. *Chem. Phys.* **1983**, *77*, 131.

(9) Miyasaka, H.; Masuhara, H.; Mataga, N. *Laser Chem.* **1987**, *7*, 119.

(10) Gauduel, Y.; Martin, J. L.; Migus, A.; Antonetti, A. In *Ultrafast Phenomena V*; Fleming and Siegman, Eds.; Springer Verlag: New York, 1986; p 308. Migus, A.; Gauduel, Y.; Martin, J. L.; Antonetti, A. *Phys. Rev. Lett.* **1987**, *58*, 1559.

(11) Ogura, H.; Hamill, W. H. *J. Phys. Chem.* **1973**, *77*, 2952.

(12) Hamill, W. H. *J. Phys. Chem.* **1969**, *73*, 1341.

\* Author to whom correspondence should be addressed.